Title
CURRENT DISTRIBUTION ON A ROTATING DISK ELECTRODE.

Author
Marathe, Vinay.

Publication Date
1968-06-01

UCRL-18264

University of California

Ernest O. Lawrence Radiation Laboratory

CURRENT DISTRIBUTION ON A ROTATING DISK ELECTRODE

Vinay Marathe

(M. S. Thesis)

June 1968

Berkeley, California

DISCLAIMER

UCRL-18264

UNIVERSITY OF CALIFORNIA

Lawrence Radiation Laboratory
Berkeley, California

AEC Contract No. W-7405-eng-48

CURRENT DISTRIBUTION ON A ROTATING DISK ELECTRODE

Vinay Marathe

(M. S. Thesis)

June 1968

TABLE OF CONTENTS

CURRENT DISTRIBUTION ON A ROTATING DISK ELECTRODE

Vinay Marathe

Inorganic Materials Research Division
Lawrence Radiation Laboratory, and
Department of Chemical Engineering
University of California, Berkeley

June 1968

ABSTRACT

The current distribution on a rotating disk electrode, for the deposition of copper, was studied experimentally for comparison with the theoretical predictions reported earlier.[13] Copper electrodes were used with copper sulfate and sulfuric acid as the electrolyte.

The experimental results were found to be in good agreement with Newman's numerical results.

INTRODUCTION

The basic theory of the rotating disk electrode was first developed and published by Levich in 1942. The hydrodynamics of a lamina rotating in an infinite medium had been solved earlier by von Kármán and Cochran.[4] Using this and assuming constant physical properties, Levich solved the convective diffusion equation for the steady state. Ever since, the rotating disk electrode has received considerable attention. More recently the transient hydrodynamic and mass transfer characteristics were studied by Olander[16], Hale[8], and Filinovskii and Kiryanov.[5] The velocity and concentration profiles, with variation in physical properties accounted for, have been recently solved by Newman and Hsueh.[15]

Now the rotating disk electrode is a versatile tool for the study of electrode processes. Among the several applications, the determination of diffusion coefficients has received the most attention. Many of the values reported are in reasonable agreement with those obtained by other methods. The diffusion coefficients obtained are integral diffusion coefficients like those from the diaphragm cell technique. The rotating disk electrode is being increasingly used for studying moderately fast electrode reactions where mass transfer plays a role in the overall rate. It has been used for studying the effect of additives and for determination of bulk concentrations. It offers some advantages over other electrode systems in studying the above mentioned and other electrochemical phenomena. First the mass transfer and hydrodynamics are well understood - this is not true of many other electrode systems. The effects of natural convection are eliminated due to the strong forced convection. In addition the current density on tne disk electrode is uniform at the limiting current.

Newman[13] has recently shown that below the limiting current the current distribution is nonuniform and is obtained by solving for the concentration and potential distribution simultaneously with electrode kinetics supplying the boundary conditions. The distribution is governed by several parameters involving the transport properties of the electrolyte, the angular velocity of the disk, and electrode kinetic constants. Newman's theory is valid for metal deposition from a single salt solution and electrode reactions with an excess of supporting electrolyte.

The aim of this work is to check Newman's theory by studying the current distribution for copper deposition from copper sulfate and sulfuric acid. The deposit thickness is measured experimentally. This should be proportional to the current density distribution if the deposit has uniform density

2. THEORY

2.1 Basic Relations:

Some basic relations pertaining to transport processes in electrolytic systems are stated here so that they can be referred to later on. Newman[14] has treated these and other fundamentals in detail in a review on transport processes in electrolytic solutions. These relations are based on the assumption of constant physical properties and the dilute solution theory.

The flux (moles/cm^{2}sec) of any component i is given by

$$\underline{N}_i = -z_i u_i F c_i \nabla\phi - D_i \nabla c_i + c_i \underline{v} \; . \tag{1}$$

On the right-hand side the three terms represent contributions due to migration, diffusion, and convection, respectively.

The current density (amp/cm^2) at any point in the system is related to the fluxes according to

$$\underline{i} = F \sum_i z_i \underline{N}_i \; . \tag{2}$$

Material balance for a species yields

$$\frac{\partial c_i}{\partial t} + \nabla \cdot \underline{N}_i = R_i \tag{3}$$

where R_i is the rate of production (moles/cm^{3}sec) of species i by homogeneous reactions. Since we are dealing with stationary processes (steady-state) and the reactions occur only at the electrodes, the above equation reduces to

$$\nabla \cdot \underline{N}_i = 0 \; . \tag{4}$$

The equation of electroneutrality

$$\sum_i z_i c_i = 0 \tag{5}$$

states that the solution is electrically neutral. This is valid everywhere in the solution except in the double layer in the immediate vicinity of the electrode.

Substituting (1) in (2) and employing (5) we get

$$\underline{i} = -F^2\nabla\phi\sum_i z_i^2 c_i u_i - F\sum_i z_i D_i \nabla c_i \ . \tag{6}$$

Employing the equation of continuity, $\nabla\cdot\underline{v} = 0$ and substituting (1) in (4) we get

$$\underline{v}\cdot\nabla c_i = D_i\nabla^2 c_i + z_i u_i F\nabla\cdot(c\nabla\phi) \ . \tag{7}$$

In Appendix A it is shown that for a binary salt the current density on the cathode is given by

$$\underline{i} = \frac{nFD}{1-t_+}\left.\frac{\partial c}{\partial y}\right|_{y=0} \tag{8}$$

and the equation of convective diffusion is

$$\underline{v}\cdot\nabla c = D\nabla^2 c \tag{9}$$

where
$$t_+ = \frac{z_+u_+}{z_+u_+ - z_-u_-} \quad \text{and} \quad D = \frac{z_+u_+D_+ - z_-u_-D_-}{z_+u_+ + z_-u_-} \tag{10}$$

and n = number of electrons produced when one ion or molecule reacts.

Relations (8) and (9) are also valid for a minor component with excess supporting electrolyte when $t_+ = 0$ and D is the ionic diffusion coefficient of the species.

2.2 Analysis:

At low currents or high rotation speeds when the mass transfer limitations are negligible, the concentrations at the disk surface do not differ from the bulk concentration. The concentration overpotential is

negligible and if we ignore surface overpotential the solution adjacent to the disk is equipotential. The current distribution can then be obtained by using (6) with $\nabla c = 0$

$$\underline{i} = -F^2 \nabla \phi \sum_i z_i^2 c_i u_i = -\kappa_\infty \left.\frac{\partial \phi}{\partial y}\right|_{y=0} \tag{11}$$

where ϕ is obtained by solving the Laplace equation (valid since $\nabla \cdot \underline{i} = 0$, charge balance) subject to boundary conditions appropriate to the geometry. This yields what is referred to as "the primary current distribution"; the current density is infinite at the edge of the disk and at the center equal to 50% of the average current density.

As opposed to this, when mass transfer is completely controlling, the reactant is used up as soon as it arrives at the electrode, and the concentration is zero everywhere on the disk. Due to this, the concentration profile can be solved without computing the potential distribution. The current distribution is then obtained by equation (8)

$$\underline{i} = \frac{nFD}{1-t_+} \left.\frac{\partial c}{\partial y}\right|_{y=0} . \tag{12}$$

This is the so-called "limiting current distribution" and, as shown later, is uniform in this case.

In the intermediate range mass transfer limitations are neither negligible nor controlling. The concentrations on the disk surface are not known and must, along with the current densities, be such that they adjust themselves to the overpotentials available after subtracting the ohmic drop (potential outside the diffusion layer) from the voltage applied to the cell. However, the potential outside the diffusion layer cannot be determined independently since the solution adjacent to the disk is not

equipotential. Hence an iterative approach, where the concentration profile in the diffusion layer and the potential outside the diffusion layer are computed simultaneously, is necessary.

2.3 Concentration Profile in the Diffusion Layer:

The concentration profile is obtained from the "equation of convective diffusion", equation (9). Since there is axial symmetry and the only dominant term on the right is the y-term, this becomes

$$v_r \frac{\partial c}{\partial r} + v_y \frac{\partial c}{\partial y} = D \frac{\partial^2 c}{\partial y^2} . \tag{13}$$

Very close to the electrode surface the velocities can be approximated by

$$v_r = ary\Omega\sqrt{\frac{\Omega}{\nu}} \quad \text{and} \quad v_y = -ay^2\Omega\sqrt{\frac{\Omega}{\nu}} \tag{14}$$

where $a = 0.51023$. It is valid to use the above approximation in the diffusion layer if it is thin compared to the momentum boundary layer i.e., if Schmidt number, $Sc = \frac{\nu}{D}$, is large. For electrolytic solutions Sc is of the order of 1000. Equation (13), after substituting for the velocities yields the following concentration profile

$$c = c_\infty \left[1 + \sum_{m=0}^{\infty} A_m (r/r_o)^{2m} \theta_m(\zeta)\right] \tag{15}$$

where

$$\zeta = y\left(\frac{a\nu}{3D}\right)^{1/3}\sqrt{\frac{\Omega}{\nu}} \tag{16}$$

and $\theta_m(\zeta)$ is obtained from

$$\theta_m'' + 3\zeta^2\theta_m' - 6m\zeta\theta_m = 0 \tag{17}$$

satisfying the boundary conditions

$$\left.\begin{aligned} \theta_m &= 1 \quad \text{at} \quad \zeta = 0 \\ \theta_m &= 0 \quad \text{at} \quad \zeta = \infty . \end{aligned}\right\} \tag{18}$$

The concentration on the disk surface will therefore be

$$c_o = c_\infty \left[1 + \sum_{m=0}^{\infty} A_m (r/r_o)^{2m}\right] \tag{19}$$

and the current density on the disk using (8) is

$$\underline{i} = \frac{nFDc_\infty}{1-t_+} \left(\frac{a\nu}{3D}\right)^{1/3} \sqrt{\frac{\Omega}{\nu}} \sum_{m=0}^{\infty} A_m (r/r_o)^{2m} \theta_m'(0). \tag{20}$$

At limiting current the concentration is zero everywhere on the disk surface. Hence, from (19), $A_o = -1$, $A_m = 0$, $m = 1,2,3.....$. The limiting current density is then obtained from (20) as

$$i_{lim} = - \frac{nFDc_\infty}{1-t_+} \left(\frac{a\nu}{3D}\right)^{1/3} \sqrt{\frac{\Omega}{\nu}}\, \theta_o'(0) \tag{21}$$

and has no radial dependence, i.e., is uniform.

2.4 Potential Distribution outside the Diffusion Layer:

Outside the diffusion layer the conductivity is constant κ_∞ (due to uniform concentration) and conservation of charge yields Laplace's equation. In rotational elliptic coordinates defined by

$$y = r_o \xi\eta \quad \text{and} \quad r = r_o \sqrt{(1+\xi^2)(1-\eta^2)}, \tag{22}$$

the Laplace equation becomes

$$\frac{\partial}{\partial\xi}\left[(1+\xi^2)\frac{\partial\phi}{\partial\xi}\right] + \frac{\partial}{\partial\eta}\left[(1-\eta^2)\frac{\partial\phi}{\partial\eta}\right] = 0. \tag{23}$$

For the rotating disk electrode, boundary conditions take the form

$$\left.\begin{aligned} &\frac{\partial\phi}{\partial\eta} = 0 \text{ at } \eta = 0 \text{ (on the insulating annulus)} \\ &\phi = 0 \text{ at } \xi = \infty \text{ (far from the disk)} \\ &\phi \text{ well behaved at } \eta = 1 \text{ (on the axis)} . \end{aligned}\right\} \tag{24}$$

The solution of (23) subject to the above conditions is

$$\phi = \frac{RT}{ZF} \sum_{n=0}^{\infty} B_n P_{2n}(\eta) M_{2n}(\xi) \tag{25}$$

where $P_{2n}(\eta) \equiv$ Legendre polynomial of order 2n

$M_{2n}(\xi) \equiv$ Legendre function satisfying

$$\frac{d}{d\xi}\left[(1+\xi^2)\frac{dM_{2n}}{d\xi}\right] = 2n(2n+1)M_{2n}$$

with the boundary conditions

$$M_{2n} = 1 \text{ at } \xi = 0 \quad \text{and} \quad M_{2n} = 0 \text{ at } \xi = \infty .$$

The ohmic drop has been non-dimensionalized with the coefficient RT/ZF for consistency with the overpotential expressions

$$\begin{aligned} Z &= -z_+z_-/(z_+-z_-) \text{ for single salt} \\ &= -n \text{ with excess supporting electrolyte .} \end{aligned} \tag{26}$$

From (25) the ohmic drop extrapolated to the disk surface, ϕ_o, is obtained by letting $\xi = 0$

$$\phi_o = \frac{RT}{ZF} \sum_{n=0}^{\infty} B_n P_{2n}(\eta) . \tag{27}$$

The current density just outside the diffusion layer will be

$$\begin{aligned} \underline{i} &= -\kappa_\infty \left.\frac{\partial \phi}{\partial y}\right|_{y=0} \\ &= -\frac{\kappa_\infty}{r_o \eta} \frac{RT}{ZF} \sum_{n=0}^{\infty} B_n P_{2n}(\eta) M'_{2n}(0) \end{aligned} \tag{28}$$

and since the diffusion layer is very thin this should be equal to the current density on the disk surface (20). This facilitates a relationship between B_n's and A_m's.

$$B_n = \frac{\pi}{4} N \sum_{m=0}^{\infty} Q_{n,m} A_m \tag{29}$$

where

$$N = \frac{nZF^2 Dc_\infty}{RT(1-t_+)_\infty} r_o \sqrt{\frac{\Omega}{\nu}} \left(\frac{a\nu}{3D}\right)^{1/3} \tag{30}$$

and

$$Q_{n,m} = (4n+1) \frac{4\theta_o'(0)}{\pi M_{2n}'(0)} \int_0^1 \eta (1-\eta^2)^m P_{2n}'(\eta) d\eta \ . \tag{31}$$

The last equation is obtained by utilizing the orthogonality of Legendre Polynomials and the fact that

$$r^2 = 1 - \eta^2 \quad \text{when} \quad \xi = 0 \text{ (on the disk).}$$

2.5 Overpotentials:

The disk being metallic must be at a constant potential V (applied voltage) given by

$$V = \phi_o + \eta_s + \eta_c \tag{32}$$

where $\phi_o \equiv$ ohmic drop, extrapolated to the disk surface

$\eta_s \equiv$ surface overpotential

and $\eta_c =$ concentration overpotential.

The concentration overpotential is given by

$$\eta_c = \frac{RT}{ZF} \left[ln\left(\frac{c_o}{c_\infty}\right) + t_+ \left(1 - \frac{c_o}{c_\infty}\right)\right] \ . \tag{33}$$

This is valid for metal deposition from a single salt and also for the reaction of a minor component with excess supporting electrolyte.

The surface overpotential is related to the surface concentration and the current density by the expression

$$\underline{i} = i_o \left(\frac{c_o}{c_\infty}\right)^\gamma \left[\exp\left\{\frac{\alpha ZF}{RT} \eta_s\right\} - \exp\left\{-\frac{\beta ZF}{RT} \eta_s\right\}\right], \tag{34}$$

where γ is the slope of a logarithmic plot of exchange current density versus concentration.

At low currents when $|i| \ll i_o$, $c_o \to c_\infty$, $\eta_c = 0$ and η_s tends to zero and the above equation yields

$$\frac{di}{d\eta_s} = i_o \frac{ZF}{RT} (\alpha+\beta) \ . \tag{35}$$

The current varies linearly with η_s and the slope is independent of the current level. This suggests the dimensionless exchange current density

$$J = i_o \frac{ZF}{RT} \frac{r_o}{\kappa_\infty} \tag{36}$$

as one of the parameters controlling the current distribution.

At higher currents when $|i| \gg i_o$ but $|i| \ll i_{lim}$, one of the exponential terms in (34) becomes negligible and

$$\eta_s = - \frac{1}{\beta} \frac{RT}{ZF} [\ln |i| - \ln i_o] \ , \tag{37}$$

i.e., η_s is no longer linearly related to the current density and the slope depends on the current level. In consistency with the earlier expression, the dimensionless average current density is defined by

$$\delta = i_{avg} \frac{ZF}{RT} \frac{r_o}{\kappa_\infty} \ . \tag{38}$$

Parameter N, defined in equation (30), may be expressed as

$$N = \frac{i_{lim}}{\theta_o'(0)} \frac{ZF}{RT} \frac{r_o}{\kappa_\infty} \tag{39}$$

and so can be considered as a dimensionless limiting current density. Newman[13] has given several plots of current and concentration distribution on the disk surface with N, J, and δ as parameters for some values of α, β, γ, and t_+ .

2.6 Equations and Computational Scheme:

The system can be represented by the following equations:

$$c_o = c_\infty \left[1 + \sum_{m=0}^{\infty} A_m (r/r_o)^{2m}\right] \qquad (a)$$

$$i = \frac{nFDc_\infty}{1-t} \left(\frac{a\nu}{3D}\right)^{1/3} \sqrt{\frac{\Omega}{\nu}} \sum_{m=0}^{\infty} A_m (r/r_o)^{2m}\, \theta_m'(0) \qquad (b)$$

$$\phi_o = \frac{RT}{ZF} \sum_{n=0}^{\infty} B_n P_{2n}(\eta) \qquad (c)$$

$$V = \phi_o + \eta_s + \eta_c \qquad (d)$$

$$\eta_c = \frac{RT}{ZF} \left[ln \left(\frac{c_o}{c_\infty}\right) + t_+\left(1 - \frac{c_o}{c_\infty}\right)\right] \qquad (e)$$

$$\underline{i} = i_o \left(\frac{c_o}{c_\infty}\right)^{\gamma} \left[\exp\left\{\frac{\alpha ZF}{RT}\, \eta_s\right\} - \exp\left\{-\frac{\beta ZF}{RT}\, \eta_s\right\}\right] \qquad (f)$$

$$B_n = \frac{\pi}{4} N \sum_{m=0}^{\infty} Q_{n,m}\, A_m \,. \qquad (g)$$

For numerical calculations all the series have to be truncated. The coefficients A_m of the concentration series (a) have alternating signs and large and considerably varying values depending on where the series is truncated. It is therefore more convenient to express the concentration in terms of Legendre polynomials

$$c_o = c_\infty \left[1 + \sum_{\ell=0}^{\infty} a_\ell P_{2\ell}(r/r_o)\right] .$$

This facilitates easy determination of the coefficients by using the

orthogonality of Legendre polynomials

$$a_\ell = (4\ell+1)\int_0^1 \left(\frac{c_o}{c_\infty} - 1\right) P_{2\ell}(r/r_o)\, d(r/r_o) \qquad (h)$$

and then A_m's can be obtained by comparing the two series.

It is seen from (19), (20), and (21) that

$$\text{at } r = 0 \qquad \frac{i}{i_{lim}} = 1 - \frac{c_o}{c_\infty} \quad .$$

The current distribution can be obtained by the iterative procedure indicated in Figure 2-1.

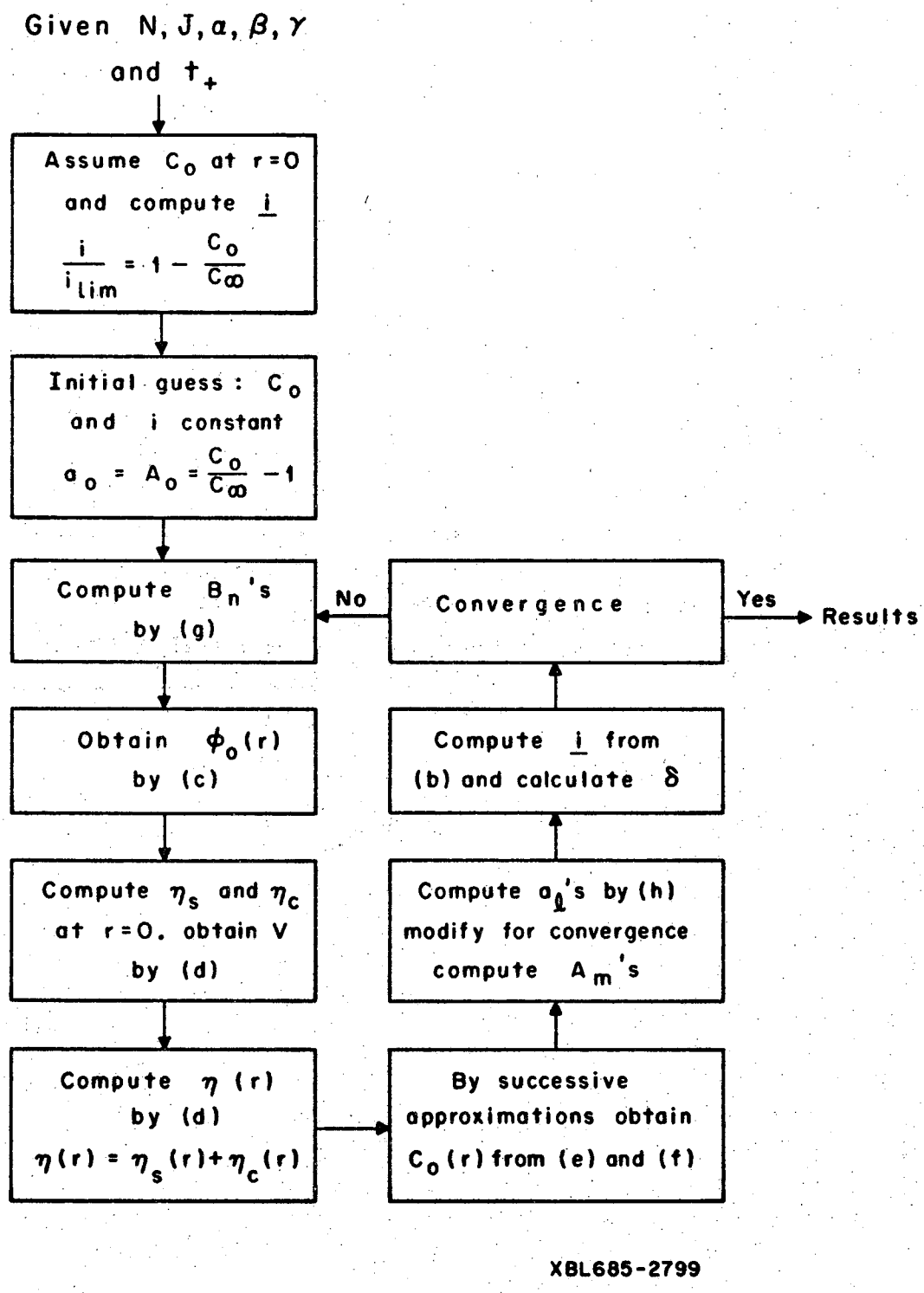

Figure 2-1. Computational Scheme.

3. DESIGN OF THE ROTATING DISK ELECTRODE

3.1 Design of the Rotating Disk Electrode

The design of the disk electrode should conform as closely as possible to the theoretical requirements. Riddiford[18], in a review on the rotating disk system, has suggested several design factors based on theoretical and experimental considerations.

First a disk of finite radius r_1 will be effective as an infinite lamina if the diameter is considerably larger than the momentum boundary layer, i.e.,

$$r_1 \gg 2.8 \left(\frac{\nu}{\Omega}\right)^{1/2} .$$

In addition to ensure that the disk will function as an infinite lamina no serious edge correction should be introduced due to the finite span of the disk, i.e., the flow in the upper half should not interfere with the flow in the lower half. To achieve this the thickness of the disk should be less than 1/30th of the disk diameter and the size of the shaft should less than 30% of the size of the disk.

Practical considerations like too small a thickness of the disk for machining and rigidity, may rule out some of the above factors. Yet it is necessary to confirm experimentally that the flow in the upper half of the system is confined to $y < 0$.

The disk should be horizontal and eccentricity (both axial and perpendicular to the disk axis) should be minimum. The disk should be smooth to the extent that rugosity is much less than the momentum boundary layer thickness to maintain the theoretically expected velocity profiles.

Fluid velocities near the disk surface can be approximated by (14)

only if the flow is laminar. Experimental studies of turbulence in the rotating disk system, enumerated by Riddiford[18], report varying values for the $Re_{(trans)}$ and $Re_{(critical)}$. (These are respectivly the values of $Re = \frac{r_o^2\Omega}{\nu}$ at which the flow ceases to be completely laminar and the Re for onset of turbulence.) Most values for Re (trans) are around 2×10^5, the lowest one being 1.8×10^5. To ensure that laminar flow prevails everywhere, the Re at the outer edge of the disk should be less than 1.8×10^5.

At lower rotation speeds when Re ~ 10 the contribution of natural convection is no longer negligible and also the momentum boundary layer becomes comparable to the disk size. To prevent these $(Re)_{avg}$ should be considerably larger than 10.

To eliminate edge effects and to avoid unprotected edges, it is desirable to use electrodes with only the central portion of the lower surface active.

There is always some distrubance to the flux at the outer edge of the working surface since the thickness of the diffusion layer beyond it is uncertain. To minimize this disturbance the radius of the working surface should be much greater than the diffusion layer thickness, i.e.,

$$r_o \gg 1.61 \left(\frac{a\nu}{3D}\right)^{1/3} \sqrt{\frac{\Omega}{\nu}} \quad .$$

The potential distribution requires a finite disk embedded in an infinite insulating plane with the counter electrode and cell walls at infinity. Riddiford claims that this is achieved by any disk satisfying the fluid flow and mass transfer requirements if the counter electrode is large enough to confine polarization to the rotating disk electrode. Recently Angell, Dickinson, and Greef[2] measured the potential distributions for disk electordes satisfying Riddiford's criteria and found the results to be in good qualitative agreement with Newman's theory.[12,13]

The shape of the electrode chosen is in conformity with the shape recommended by Riddiford and other workers.

3.2 Design of the Cell

Theoretical analysis assumes that all bounding surfaces - liquid-air surface, walls of the cell and the counter electrode - are at infinite distance from the rotating disk electrode. According to Gregory and Riddiford[7] this requirement is satisfied when the bounding surfaces are 0.5 cm from the rotating disk electrode.

Kreith et al[10] studied the effect of varying the separation of a shroud from the disk on the mass transfer from napthalene disks rotating in air. With mass transfer rates expressed by the ratio of Sherwood number observed for a given separation, Sh, to the theoretical value for infinite separation, Sh_∞, they found that

$$\frac{Sh}{Sh_\infty} = 0.9 \quad \text{when} \quad y/2r_o = 0.2.$$

The cell dimensions satisfy the above requirements. It was observed that for larger electrodes than those used in this work there was considerable swirling and vortex formation. This could be avoided by using baffles or increasing the cell size on the basis of dimensional analysis.

3.3 Electrode and Cell Specifications:

The cell is made of Lucite and is 14 cm in diameter and 10 cm in height. It has a circular inset in the bottom for the counter electrode (copper: diameter 7.5 cm) to which the electrical connection can be screwed on. The cell is held to the lid by five screws. The lid is attached to the motor-shaft-spindle assembly and has openings for thermometer

and reference electrodes.

The rotating disk electrode dimensions are shown in Figure 3-1. These dimensions conform, as closely as possible, to all the factors mentioned earlier. For the copper sulfate-sulfuric acid system (in the range of concentrations employed)

ν = Kinematic viscosity $\approx 10^{-2}$ cm^2/sec

D = Diffusivity $\approx 6 \times 10^{-6}$ cm^2/sec

Ω = Rotation speed $\approx$ 10 to 31.42 radians/sec.

The disk electrode is shown in Figure 3-2. The central copper portion is machined to dimensions and cast in epoxy resin (composition mentioned in section 4.3). The epoxy is then machined on a lathe to the shape and dimensions indicated in Figure 3-1.

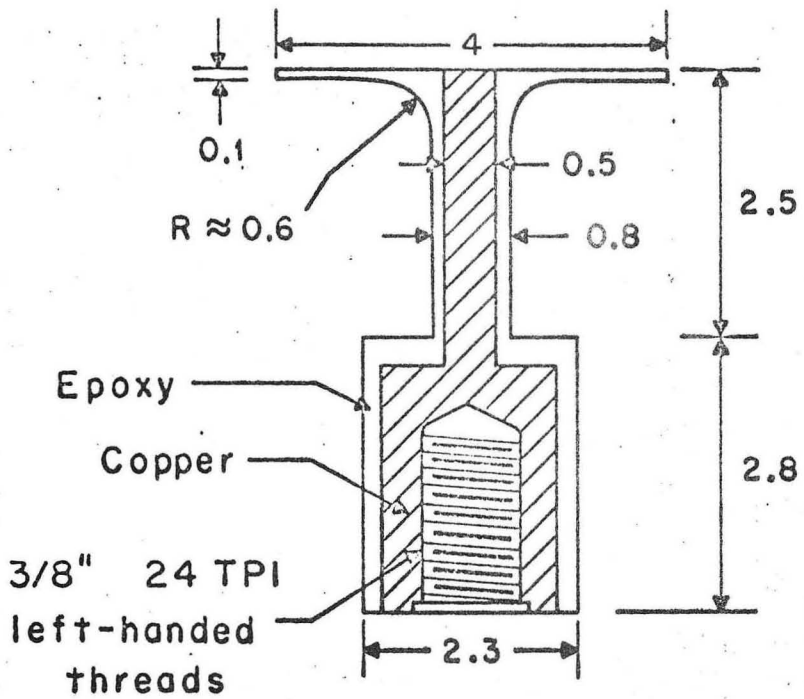

Figure 3-1. The rotating disk electrode.
All dimensions in cm.

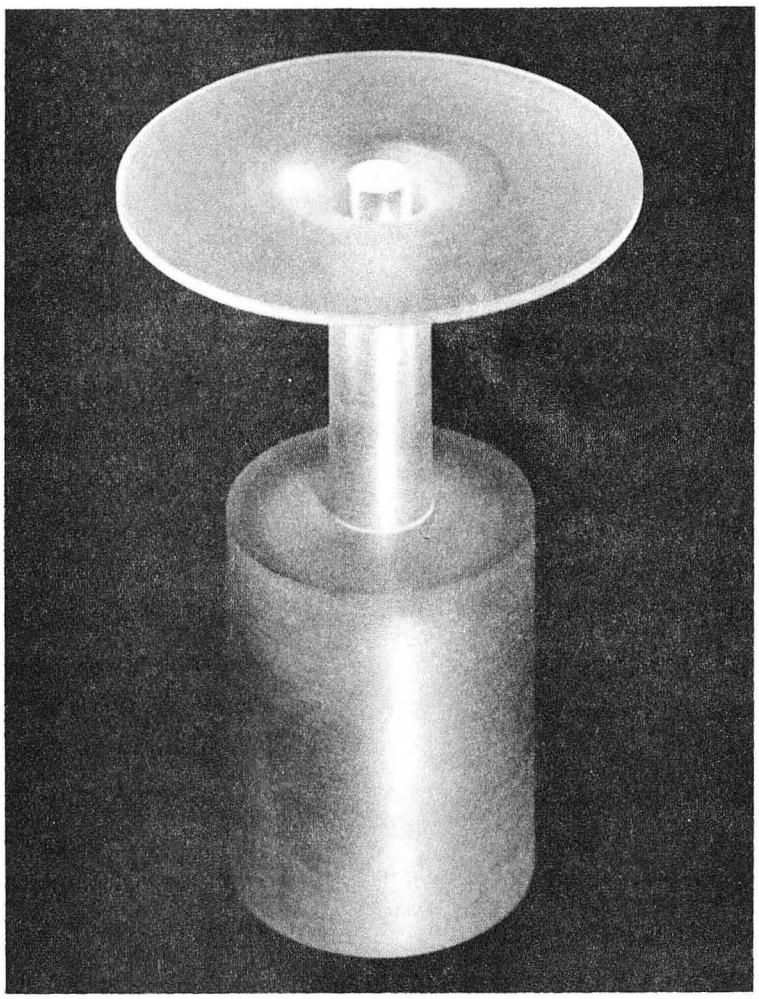

XBB 686-3955

Fig. 3-2. The rotating disk electrode

4. EXPERIMENTAL WORK

4.1 Experimental Setup:

A constant current (DC) was supplied by a Lambda Model 2B regulated power supply. The current was measured with a Keithley Model 610R Electrometer to an accuracy of 2%.

The electrical connection to the rotating disk electrode was achieved by means of a mercury well. The disk was mounted on a spindle and held there by 3/8" 24 TPI left-handed threads. The spindle was tightly filled in two 7/8-inch o.d. New Departure RC bearings. The bearings were mounted to a heavy brass bearing case in order to keep the eccentricity to a minimum. Gordon[6] has discussed the spindle assembly in great detail. The spindle was coupled to the shaft of a variable speed motor (Bodine Electrical Company, Type NSE 11R, with a gear ratio 10:1) controlled by a precision DC voltage power supply. The speed of rotation was determined by a General Radio Type 631-BL strobotac with an accuracy of about 1%.

The temperature was maintained at 25±0.1°C by immersing the cell in a water bath controlled at 25±0.1°C.

4.2 Experimental Procedure:

As stated earlier the rugosity of the disk surface should be considerably less than the momentum boundary layer thickness in order to maintain the expected velocity profiles. The momentum boundary layer varies in thickness with the transport properties of the electrolyte and the rotation speed; for the solutions and rotation speeds employed it was equal to or more than 5×10^{-2} cm. Consequently the disk electrode has to be subjected to the following surface treatment:

1. The electrodes were polished successively on #0, #00, #000, and #0000 emery paper using kerosene as a lubricant. The last paper has a grain size of 15 to 20μ.

2. The electrodes were polished on a wheel mounted with canvas cloth (Diamond Abrasive 1μ) at moderate speeds with kerosene as a lubricant.

3. If necessary the electrodes were polished on a wheel mounted with Microcloth using γ-Alumina (0.05μ) as the grinding compound.

4. Electrode surface was cleaned with isopropyl alcohol or carbon tetrachloride.

5. The electrode is rinsed with distilled water followed by the electrolyte to be used in the cell.

The disk electrode was then mounted on the spindle and the cell assembled. The system was left in the bath for a few hours until it attained the temperature of the bath (25±0.1°C).

The conditions for deposition are chosen such that the expected current distribution is fairly nonuniform and the deposit is quite smooth. For instance, with only copper sulfate, the deposit is so rough that it is difficult to characterize the deposit thickness at a point. With considerable excess of sulfuric acid the distribution is not sufficiently nonuniform for measuring the variation in deposit thickness well enough. The concentration of the electrolyte was therefore chosen to be 0.1M sulfuric acid. As in many other areas, data are comparatively plentiful at 25°C and so the experiments were done at this temperature. If the deposit is not very thin compared to the momentum boundary layer the veloctiy profile and consequently the current distribution might be altered. So

once a value is selected for the average current density the time of deposition is computed such that the maximum deposit thickness is less than 2×10^{-3} cm (momentum boundary layer thickness $\approx 5 \times 10^{-2}$ cm).

The rotation speed is set to the desired value by controlling the DC voltage supply to the motor. The current to the cell is set to the selected value and deposition done for the estimated time. Deposition times were 15 to 30 minutes.

4.3 Measurement of Deposit Distribution

Possibilities of employing conventional non-destructive testing methods for measuring thin film thicknesses were investigated.

Tolansky[20] has reported that films slightly less than a microinch can be measured to an accuracy of 1% by interferometry. He also reports that films down to 1/25th of a microinch could be measured by this technique with some loss of accuracy. There is, however, one requirement - that the deposit be bright and smooth. For the example reported he had fluoride additives in a chloride bath. No additives can be employed in the present work since these may alter transport properties and electrode kinetic parameters. The deposits were fairly bright but not smooth enough to give an interference pattern. Consequently this approach had to be abandoned.

Radiographic methods pose both theoretical and practical problems. The disk size is comparable to the size of the counter window and hence an elaborate procedure employing a set of lead plates with circular openings of various sizes would be necessary. In addition since the amount of copper deposited is so small a very high initial source activity would be necessary to minimize the statistical errors inherent in radiation

intensity measurements.[3] As a result this approach was also given up.

Other methods are not accurate enough for our purpose - for instance, ultrasonic testing methods - or are too involved and require that the film and base metal have considerably different properties - for instance, eddy-current-testing requires considerably different conductivities (here again the small size of the disk electrode would pose some problems).

In this work the distribution of the deposit was observed optically by sectioning the electrode at a plane passing through its axis. Before machining it down to the axis the electrode is embedded in epoxy resin to prevent burring of the deposit.

The disk electrode, after depositing copper at the desired conditions, was washed with water followed by isopropyl alcohol. It was then embedded in an epoxy resin made up of

100 parts by weight Resin 826 (Shell Chemical Company)

10 parts by weight LP 3 (Accelerator, Thiokol Chemical Company)

15 parts by weight D 40 (Catalyst, Furane Plastics Company)

and cured for 16 hours at 65°C after pumping down in a vacuum to eliminate bubbles and gaps at boundaries. It was then mounted on a brass stud (3/8 inch 24 TPI left-handed threads) and machined on a lathe. One-half was then machined off on a milling machine leaving about 5/1000 inch for polishing and etching. Figure 4-1 shows a sectioned electrode after polishing.

The sectioned electrode was polished on emergy paper followed by diamond on canvas cloth wheel and γ-Alumina on microcloth wheel as described in surface treatment. It was then etched so that the deposit could be distinguished from the electrode due to difference in grain structure.

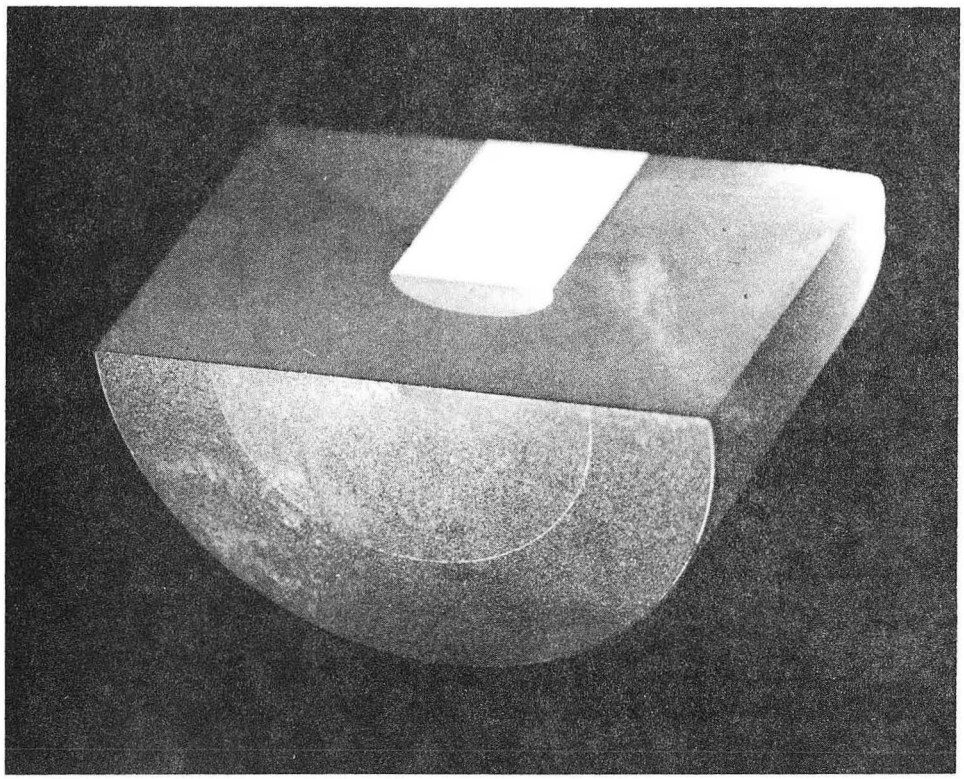

XBB 686-3956

Fig. 4-1 Sectioned electrode after polishing.

The etchant used was: 50 parts water, 50 parts ammonium hydroxide and 20 parts of 30% hydrogen peroxide.

The deposit was then observed with a metallographic microscope and microphotographs (magnification of 1000) of the deposited layer obtained at various points by a Polaroid Camera attached to the Metallograph. From these microphotographs the thickness at various points was obtained and as stated earlier (t/t_{avg}) vs (r/r_o) should coincide with (i/i_{avg}) vs (r/r_o).

5. RESULTS AND CONCLUSIONS

The theoretical current distribution is specified if the parameters N, J, δ, α, β, γ and t_+ are known. However, as shown in the computational scheme, it is easier to assume c_o at r = 0, obtain the distribution, and then compute δ. Thus only N, J, α, β, γ , and t_+ need be known.

N and J involve physical properties, like ν, κ_∞, D, transference number t_+, and exchange current density i_o. The physical properties were obtained from a correlation for physical properties of the copper sulfate-sulfuric acid system by Selman, Hsueh, and Newman.[19] The conductivities were obtained from data reported by Richardson and Taylor.[17]

For computing N by (30) the transference number t_+ should be known. If considerable excess of sulfuric acid is present, $t_+ = 0$. For copper sulfate only, $t_+ = 0.363$ (at 0.1M copper sulfate), and data for the intermediate range is lacking. The only other place where t_+ enters the computations is for obtaining the concentration overpotential, η_c, by equation (33). Concentration overpotentials are negligible at low currents and small compared to the ohmic drop and surface overpotential near limiting current. Consequently an error in t_+ will not affect the result appreciably through η_c. However if the dimensionless limiting current density, N, is computed on the basis of an erroneous t_+ it will alter the results considerably. For this reason N was computed according to (39) using the limiting current density data obtained by Selman (unpublished). For 0.1M copper sulfate and 0.1M sulfuric acid at 300 rpm the limiting current density was observed to be 65 mA/cm^2. From equation (21) and this value, the transference number was calculated to be 0.2444. It is considered desirable to use this value rather than $t_+ = 0$ for calculating concentration overpotentials.

The data on exchange current densities are quite scarce for the concentration range used in this work. Mattsson and Bockris[11] have reported exchange current densities but at higher concentration. If these data are extrapolated to 0.1M copper sulfate-0.1M sulfuric acid, we get an exchange current density of about 1 mA/cm^2. This is in fairly good agreement with values obtained from the data reported by Tor Hurlen[21] and Karasyk and Linford[9]. The value of γ, the slope of log i_o versus log c curve, was also obtained from the data of Mattsson and Bockris[11] and found to be 0.42 (however, they state that their data would yield a value of 0.6).

The electrode kinetic parameters α and β were obtained from Mattsson and Bockris[11]. They have reported values at several concentrations and concluded that within limits of reproducibility

$$\alpha Z = \alpha_a = 1.5 \quad \text{and} \quad \beta Z = \alpha_c = 0.5.$$

Shown in Figure 5.1* are microphotographs of the deposit at several points along a radius of the disk electrode. From these the thickness, average thickness, and (t/t_{avg}) are obtained. Tabulated below are results obtained from similar microphotographs.

---

* Figure 5-1: Microphotographs (≈ x 1000) of the deposit at various points when N = 22.2, J = 0.382, α = 0.75, β = 0.25, γ = 0.42, δ = 12.3

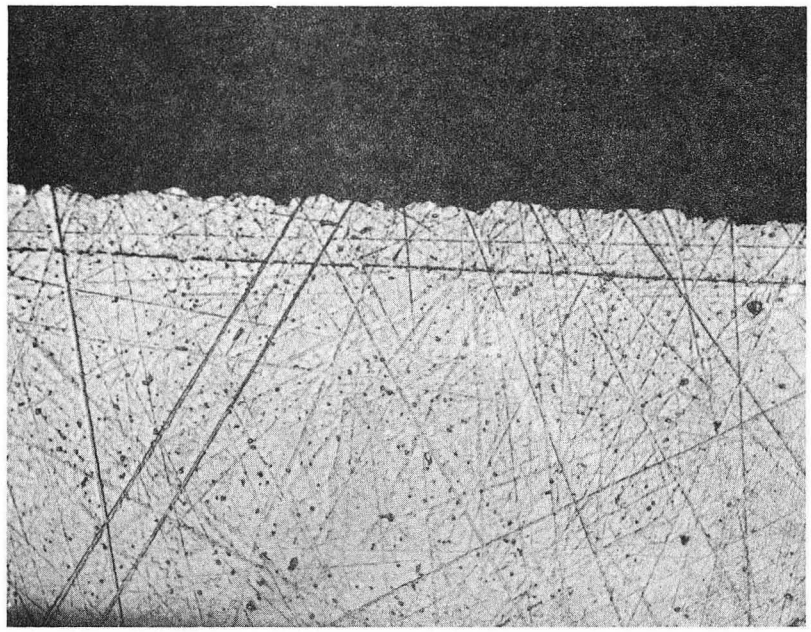

XBB 686-3957

Fig. 5-1a Deposit at $r/r_o = 0.$

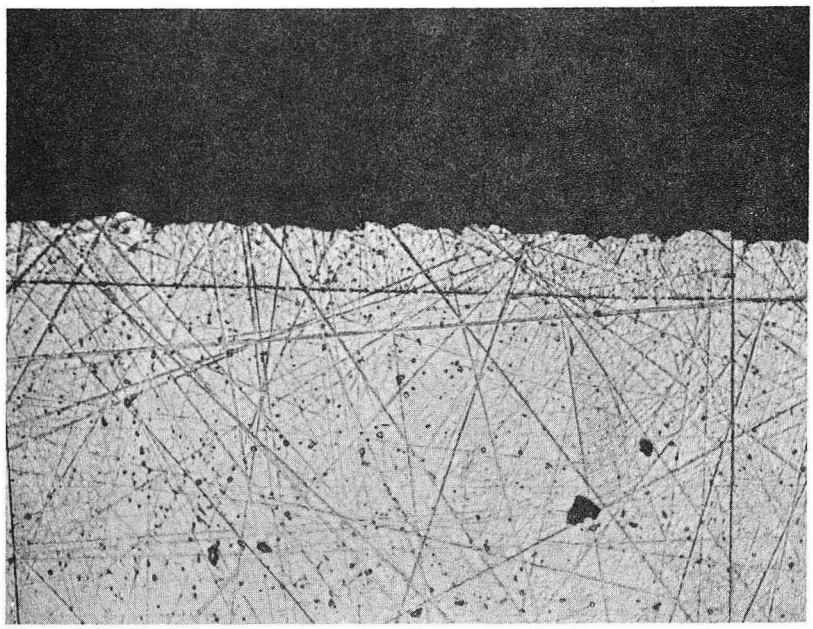

XBB 686-3958

Fig. 5-1b Deposit at $r/r_o = 0.2.$

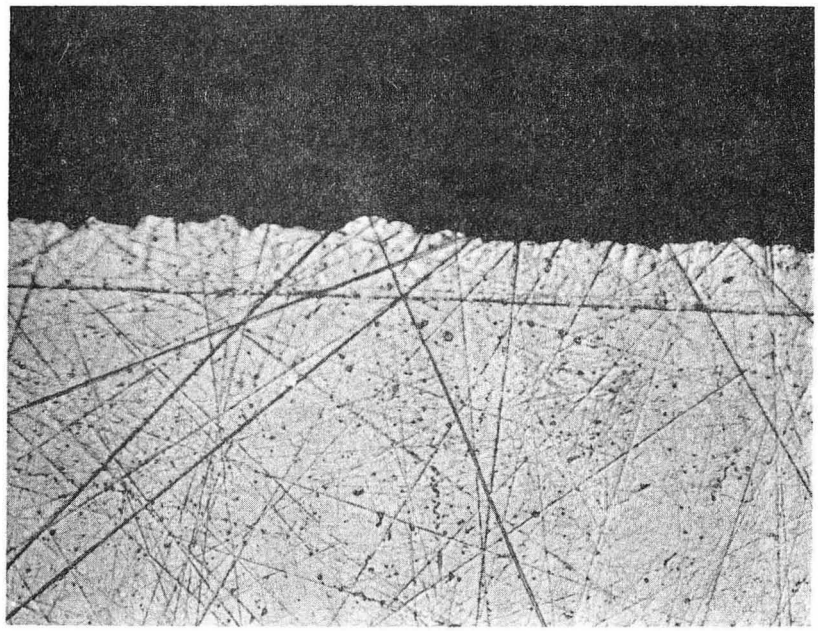

XBB 686-3959

Fig. 5-1c Deposit at $r/r_o = 0.4$.

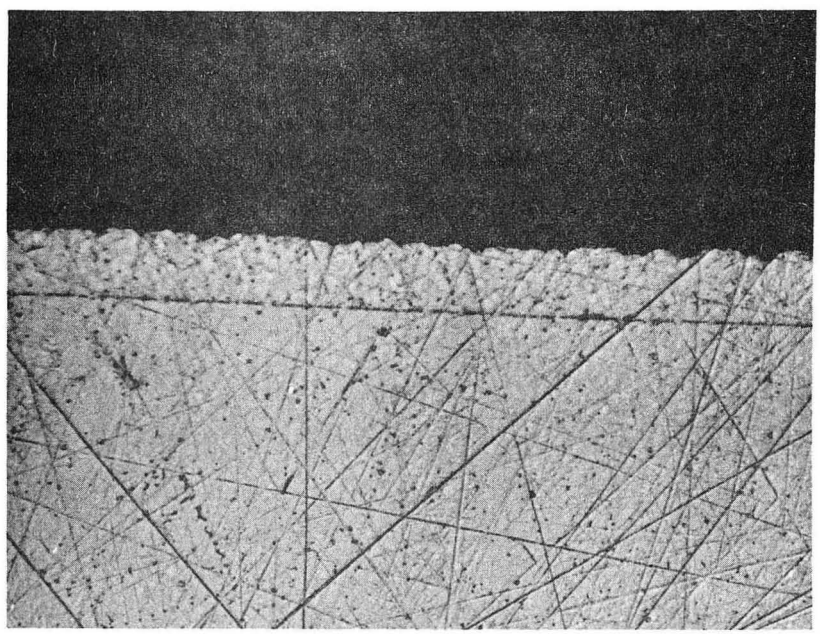

XBB 686-3960

Fig. 5-1d Deposit at $r/r_o = 0.6$.

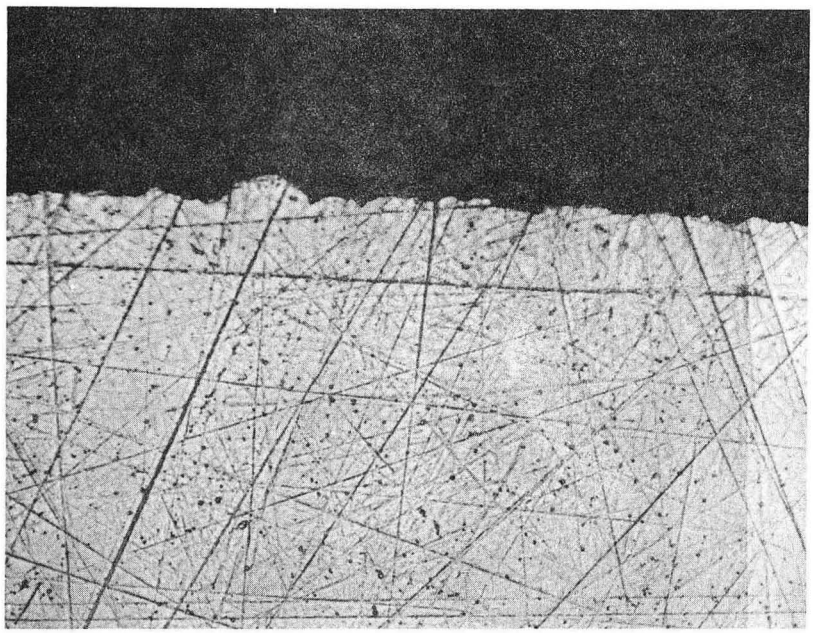

XBB 686-3961

Fig. 5-1e Deposit at $r/r_o = 0.8$.

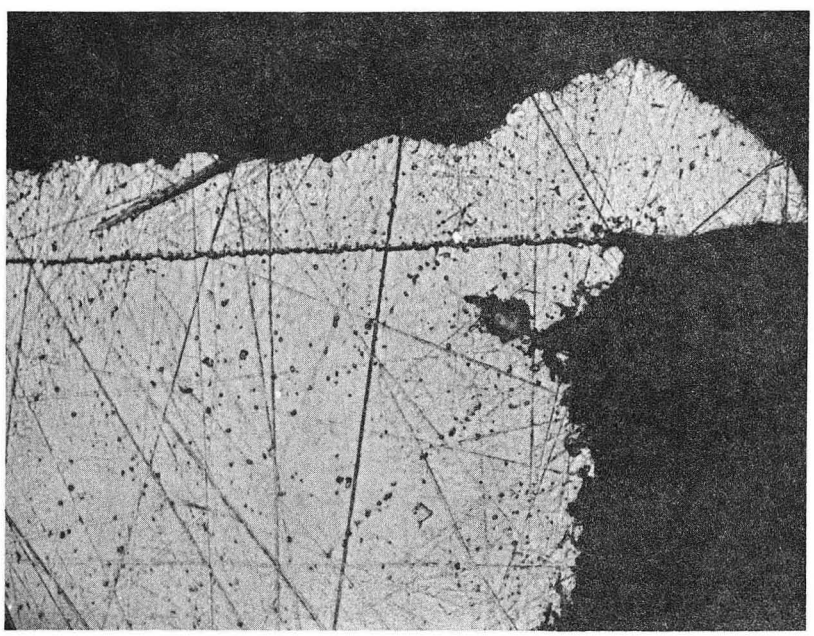

XBB 686-3962

Fig. 5-1f Deposit at $r/r_o = 1.0$.

Electrolyte: 0.1M copper sulfate - 0.1M sulfuric acid.

$T = 25°C \quad \Omega = 300$ rpm $\quad r_o = 0.25$ cm

$Z = 2$, $\kappa_\infty = 0.051$ ohm^{-1}cm^{-1}, $\nu = 0.9439 \times 10^{-2}$ cm^2/sec

$N = 22.2$, $J = 0.382$, $\alpha = 0.75$, $\beta = 0.25$

$\gamma = 0.42$, $i_{lim} = 65$ mA/cm^2

(t/t_{avg})

r/r_o	$\delta = 4.82$ 19.4% of i_{lim}	$\delta = 12.3$ 49.5% of i_{lim}	$\delta = 17.12$ 69% of i_{lim}
0	0.8367	0.7417	0.7655
0.2	0.8571	0.7748	0.8078
0.4	0.8816	0.8165	0.8481
0.6	0.945	0.8912	0.9079
0.8	1.0165	1.0022	1.006
1.0	1.323	1.7024	1.465

These results are plotted along with the theoretical current distribution obtained from Newman's theory in Figures 5-2, 3, 4. Measurements closer to the limiting current density were rendered difficult due to powdery deposits; in some cases to the extent that the deposit is partly washed away while rinsing the electrode after deposition.

Recently Albery and Ulstrup[1] have reported their experimental work with ring-disk electrodes. The electrolyte is $NaBr/HClO_4$ and the ring electrode is at such a potential that all the intermediate reaching it is destroyed. The intermediate is produced at the disk. They have shown that the ring current depends on the geometry of the electrodes and the concentration profile of the intermediate at the outer edge of the disk. They employed Newman's results[13] for the latter. This is not justified since their system does not satisfy one of the basic requirements of

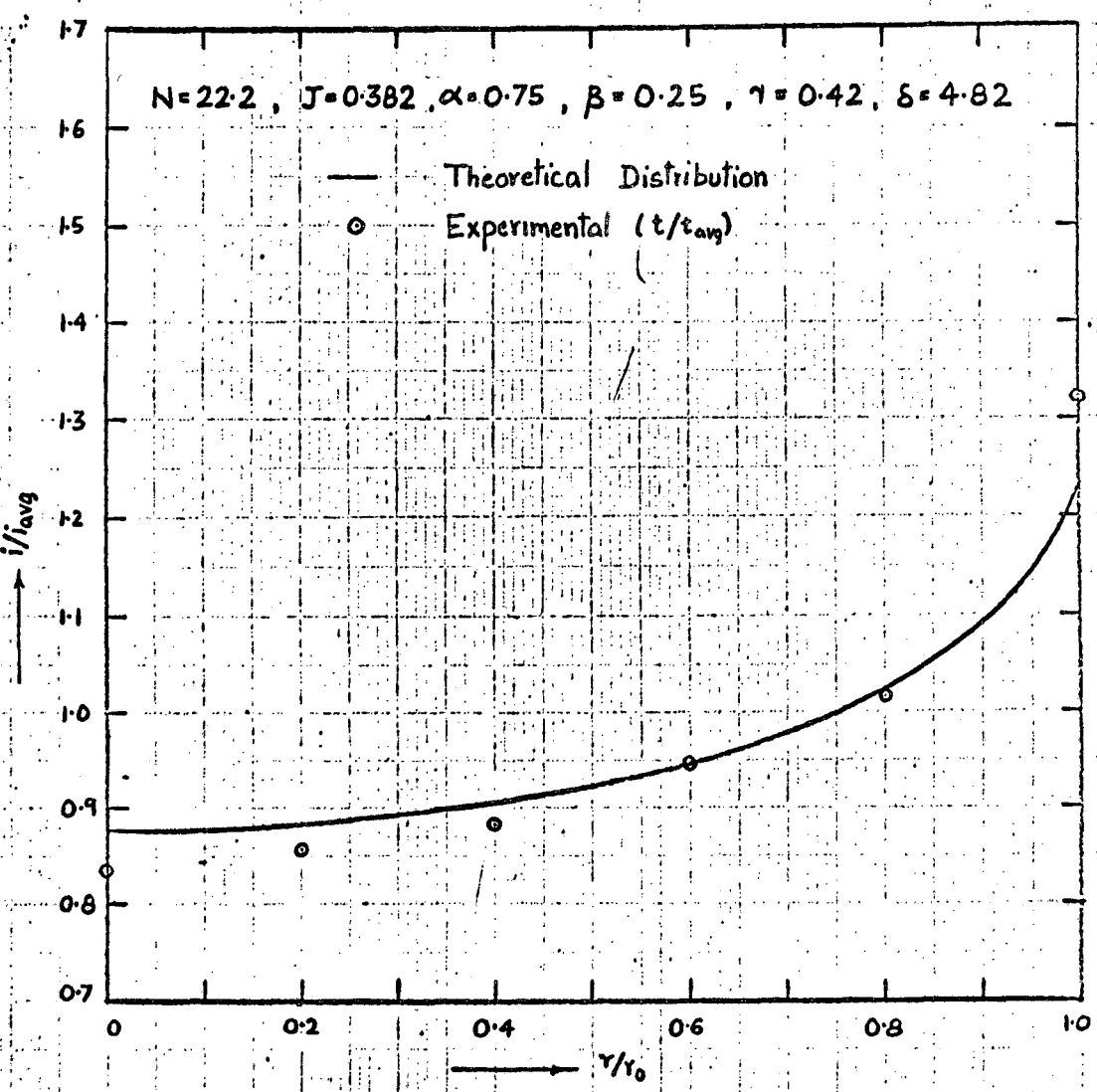

FIG. 5-2 : Current distribution at 19·4 % of the limiting current density

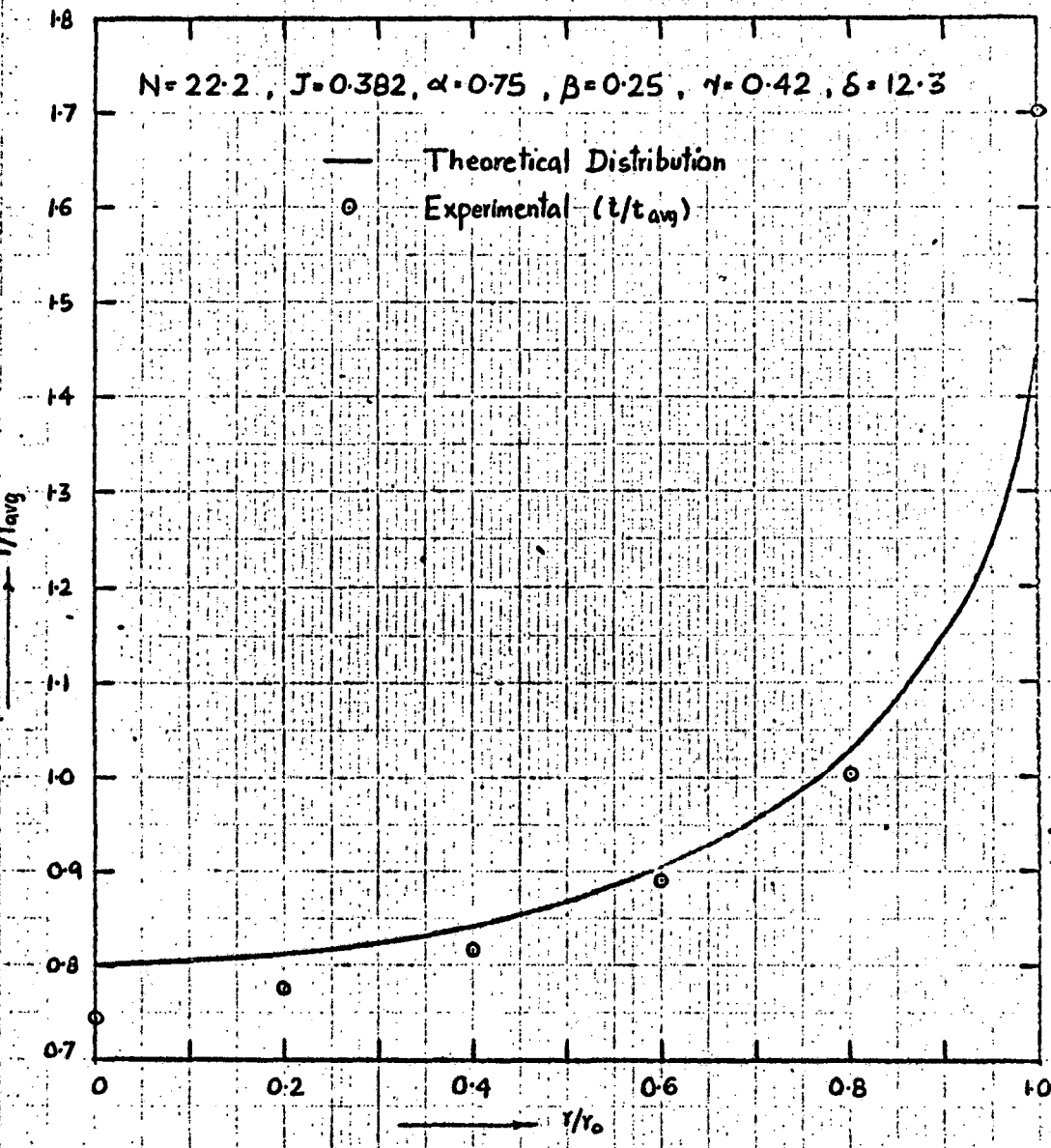

FIG. 5-3: Current distribution at 49·5% of the limiting current density

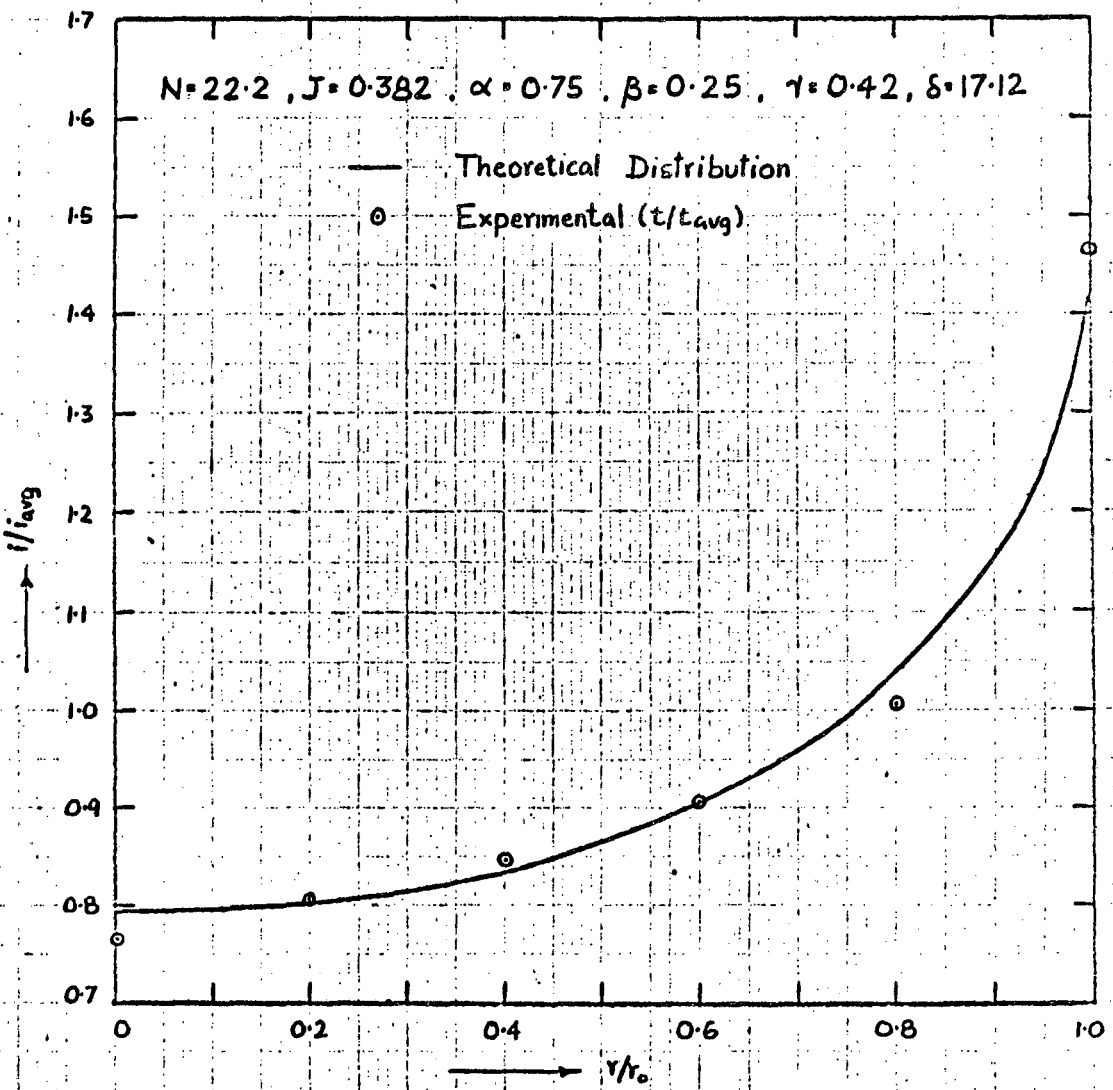

FIG: 5-4 : Current distribution at 69% of the limiting current density

Newman's theory - that the disk is imbedded in an infinite insulating plane. However, Albery and Ulstrup postulate that the discrepancies between their experimental results and Newman's numerical results may be due to the omission of the migration term in the convective diffusion equation by Newman.

The experimental method in this work is a direct approach to testing Newman's theory[13], and the results seem to confirm it within the limits of experimental accuracy.

ACKNOWLEDGEMENTS

I wish to express my deep gratitude to Professor John Newman for his guidance at every stage in the project. I also wish to express my appreciation to Mrs. Jane Schroeder for typing the final manuscript.

This work was done under the auspices of the United States Atomic Energy Commission.

APPENDIX

Here we show how relations (8) and (9) are developed for a binary salt.

If a molecule of the salt dissociates into ν_+ cations and ν_- anions

$$c = \frac{c_+}{\nu_+} = \frac{c_-}{\nu_-}$$

and $$z_+\nu_+ + z_-\nu_- = 0 .$$

Writing equation (7) for the cation and anion we get

$$\underline{v}\cdot\nabla c = z_+u_+F\nabla\cdot(c\nabla\phi) + D_+\nabla^2c$$

$$\underline{v}\cdot\nabla c = z_-u_-F\nabla\cdot(c\nabla\phi) + D_-\nabla^2c .$$

Subtracting one from the other and substituting for $\nabla\phi$ in any one of them gives

$$\underline{v}\cdot\nabla c = D\nabla^2c$$

where $$D = \frac{z_+u_+D_- - z_-u_-D_+}{z_+u_+ - z_-u_-} .$$

The current density on the cathode is given by

$$\underline{i} = -z_+FN_+ = z_+^2u_+F^2\nu_+c\nabla\phi + z_+FD_+\nu_+\nabla c .$$

The convection term vanishes since the velocity normal to the electrode is zero on the surface.

In the diffusion layer

$$\underline{i} = F^2c\nabla\phi(z_+^2u_+\nu_+ + z_-^2u_-\nu_-) + F\nabla c(z_+\nu_+D_+ + z_-\nu_-D_-) .$$

Here the convection term vanishes due to electroneutrality. Subtracting the two equations and substituting for $\nabla\phi$ in the earlier one we get

$$\underline{i} = -\frac{z_+^2u_+\nu_+F^2cD_-\nabla c}{z_-u_-cF} + z_+FD\nu_+\nabla c$$

$$\underline{i} = \frac{z_+u_+D_- - z_-u_-D_+}{z_-u_-} z_+\nu_+F\nabla c$$

$$t_+ = \frac{z_+u_+}{z_+u_+ - z_-u_-}$$

$$\frac{D}{1-t_+} = \frac{z_+u_+D_- - z_-u_-D_+}{- z_-u_-} .$$

Hence $$i = \frac{nFD}{1-t_+} \nabla c .$$

These are also valid for a minor component with supporting electrolyte when $t_+ = 0$ and D is the ionic diffusion coefficient of the reacting species.

NOMENCLATURE

a	0.51023
a_ℓ	coefficients in series for surface concentration
A_m	coefficients in series for concentration profile
B_n	coefficients in series for potential distribution
c	concentration of reactant, mole/cm^3
c_i	concentration of species i, mole/cm^3
c_o	concentration at the disk surface, mole/cm^3
c_∞	bulk concentration, mole/cm^3
D	diffusion coefficient, cm^2/sec
F	Faraday's constant, coulomb/equiv
i	normal current density at electrode surface, amp/cm^2
i_o	exchange current density, amp/cm^2
i_{avg}	average current density, amp/cm^2
i_{lim}	limiting current density, amp/cm^2
J	dimensionless exchange current density, see (36), (37)
$\bar{k}_c$	average mass transfer coefficient
n	number of electrons produced when one reactant ion or molecule reacts
N	dimensionless limiting current density, see (30), (39), (40)
N_i	flux of species i, mole/cm^2-sec
r	radial coordinate, cm
r_o	radius of the active surface of the disk, cm
r_1	radius of the disk, cm
R	universal gas constant, joule/mole-deg
$Re = \frac{r_o^2\Omega}{\nu}$	, Reynolds number

$Sc = \nu/D$, Schmidt number

$\overline{Sh} = \frac{\overline{k_c} r_o}{D}$, Sherwood number

t_+ transference number of reactant

t deposit thickness at a point

t_{avg} average deposit thickness over the disk electrode

T absolute temperature, °K

$\underline{v}$ bulk velocity vector, cm/sec

v_r, v_y velocity components, cm/sec

u_i mobility of species i, cm^2-mole/joule-sec

V potential of the disk electrode, volt

y coordinate normal to the disk, cm

z_i charge number of species i

Z see (26)

α, β, γ kinetic parameters, see (34)

δ dimensionless average current density, see (38)

ζ dimensionless normal distance, see (16)

η elliptic coordinate, see (22)

η_c concentration overpotential, volt

η_s surface overpotential, volt

θ_m functions in series for concentration profile

κ_∞ bulk conductivity, $ohm^{-1}cm^{-1}$

ν kinematic viscosity, cm^2/sec

ξ elliptic coordinate, see (22)

ϕ electrostatic potential, volt

ϕ_o potential extrapolated to disk surface, volt

Ω angular velocity, radians/sec.

REFERENCES

1. W. J. Albery and J. Ulstrup. "The Current Distribution on a Rotating Disk Electrode." Electrochimica Acta, 13, 281-284 (1968).

2. D. H. Angell, T. Dickinson, and R. Greef. "The Potential Distribution near a Rotating Disk Electrode." Electrochimica Acta, 13, 120-124 (1968).

3. J. F. Cameron. "The Uses of Radioactive Isotopes in Non-Destructive Testing." Progress in Non-Destructive Testing, 2, 91-164 (1960).

4. W. G. Cochran. "The Flow Due to a Rotating Disc." Proc. Cambridge Phil. Soc., 30, 365-375 (1934).

5. V. Y. Filinovskii and V. A. Kiryanov. "Contribution of the Theory of Nonstationary Convective Diffusion Near a Rotating Disk Electrode." Doklady Physical Chemistry, 156, 650-653 (1964). [Doklady Akad. Nauk SSSR, 156, 1412 (1964).]

6. S. L. Gordon. "Investigation of Ionic Diffusion and Migration by a Rotating Disk Electrode." Technical Report #1, Contract #DA36-039 SC-89153,45-49 (1963).

7. D. P. Gregory and A. C. Riddiford. "Transport to the Surface of a Rotating Disc." J. Chem. Soc., 3756-3764 (1956).

8. J. M. Hale. "Theory of Galvanostatic and Galvanostatic with Current Reversal Transients at a Rotating Disk Electrode." J. Electroanal. Chem., 6, 187-197 (1963).

9. L. Korasyk and H. B. Linford. "Electrode Kinetic Parameters for Copper Deposition on Clean and Soiled Copper Cathodes." J. Electrochem. Soc., 110, 895-904 (1963).

10. F. Kreith, J. H. Taylor, and J. P. Chang. "Heat and Mass Transfer from a Rotating Disk." J. Heat Transfer, 81, 95-105 (1959).

11. E. Mattsson and J. O'M. Bockris. "Galvanostatic Studies of the Kinetics of Deposition and Dissolution in the Copper + Copper Sulphate System." Trans. Faraday Soc., 55, Part 9, 1586-1601 (1959).

12. John Newman. "Resistance for Flow of Current to a Disk." J. Electrochem. Soc., 113, 501-502 (1966).

13. John Newman. "Current Distribution on a Rotating Disk below the Limiting Current." J. Electrochem. Soc., 113, 1235-1241 (1966).

14. John Newman. "Transport Processes in Electrolytic Solutions." Advances in Electrochemistry and Electrochemical Engineering, 5, 87-135 (1967).

15. John Newman and Limin Hsueh. "The Effect of Variable Transport Properties on Mass Transfer to a Rotating Disk." Electrochim. Acta, 12, 415 (1967).

16. D. R. Olander. "Unsteady-state Heat and Mass Transfer in the Rotating Disk Revolving Fluid System." Intern. J. Heat and Mass Transfer, 5, 825-836 (1962).

17. H. K. Richardson and F. D. Taylor. "The Conductivity of Mixtures of Copper Sulphate and Sulphuric Acid." Trans. Electrochem. Soc., 20, 179-184 (1911).

18. A. C. Riddiford. "The Rotating Disk System." Advances in Electrochemistry and Electrochem. Eng., 5, 47-116 (1966).

19. J. R. Selman, Limin Hsueh and John Newman. "Physical Properties of $CuSO_4$-H_2SO_4 Solutions." UCRL-17330, 49 (1966).

20. S. Tolansky. "Some Applications of Interferometry to the Examination of an Electrodeposited Film." J. Electrodepositor's Tech. Soc., 27, 171-181 (1951).

21. Tor Hurlen. "On the Kinetics of the Cu/Cu^{++}_{aq} Electrode." Acta Chem. Scand., 15, 630-644 (1961).